



HAL
open science

COVID-19 Calls for Mathematics, Part 2: Interleukin IL-6 and Myo-Inositol, Suicide-substrate Enzyme Inhibitors

Paolo Bernuzzi, Rachele Esposito, Corrado Mascia, Alessandra Massimi, Francesca Pallicca, Alessio Sanna, Chiara Simeoni

► **To cite this version:**

Paolo Bernuzzi, Rachele Esposito, Corrado Mascia, Alessandra Massimi, Francesca Pallicca, et al.. COVID-19 Calls for Mathematics, Part 2: Interleukin IL-6 and Myo-Inositol, Suicide-substrate Enzyme Inhibitors. *Organisms. Journal of Biological Sciences*, 2020, 4 (1), pp.128-139. 10.13133/2532-5876/16969 . hal-03032440

HAL Id: hal-03032440

<https://hal.science/hal-03032440v1>

Submitted on 30 Nov 2020

HAL is a multi-disciplinary open access archive for the deposit and dissemination of scientific research documents, whether they are published or not. The documents may come from teaching and research institutions in France or abroad, or from public or private research centers.

L'archive ouverte pluridisciplinaire **HAL**, est destinée au dépôt et à la diffusion de documents scientifiques de niveau recherche, publiés ou non, émanant des établissements d'enseignement et de recherche français ou étrangers, des laboratoires publics ou privés.

Special Issue: Sars-CoV-2 Epidemic

Vol. 4, No. 1 (2020)
ISSN: 2532-5876
Open access journal licensed under CC-BY
DOI: 10.13133/2532-5876/16969

COVID-19 Calls for Mathematics, Part 2: Interleukin IL-6 and Myo-Inositol, Suicide-substrate Enzyme Inhibitors

Paolo Bernuzzi^a, Rachele Esposito^a, Corrado Mascia^{a}, Alessandra Massimi^a, Francesca Pallicca^a, Alessio Sanna^a
and Chiara Simeoni^b*

^a *Dipartimento di Matematica, G. Castelnuovo, Sapienza Università di Roma*

^b *Laboratoire de Mathématiques, J.A. Dieudonné CNRS UMR 7351, Université Côte d'Azur, Parc Valrose, 06108 Nice Cedex 2, France*

***Corresponding authors:** Corrado Mascia, corrado.mascia@uniroma1.it, Chiara Simeoni, chiara.simeoni@univ-cotedazur.fr

Abstract

Interleukin IL-6 is a cytokine produced in response to various types of damage (infections, tissue injuries, autoimmune diseases, etc.) whose action contributes to host defense through stimulation of acute phase responses and immune reactions. However, experimental data show that high concentration levels of interleukin IL-6, and the subsequent inflammatory cascade induced into the organisms, could lead to several complications, such as organs progressive deterioration. The abnormal release of interleukin IL-6 is also a consequence of SARS-CoV-2 virus contagion, usually causing interstitial pneumonia and respiratory failure, which appear to be the source of decease in most of patients. Tocilizumab and myo-Inositol are two possible remedies proposed in the clinical literature to contrast the uncontrolled synthesis of interleukin IL-6, although the former exhibits non negligible collateral effects, differently from the latter. For this reason, the mathematical investigation of myo-Inositol interaction with other relevant substances involved in the SARS-CoV-2 could support the bio-medical research in determining, the optimal doses and administration timing necessary to minimize damages, in order to support the clinical results. The preliminaries of this approach are the subject of this article.

Moreover, because a vaccine against the SARS-CoV-2 virus will not be available shortly, we consider another possible pharmacological strategy to contrast its activity. There exist several candidate medicines which may inhibit infection and replication of SARS-CoV-2, and we focus our attention on the process of enzymatic inhibition through mechanism-based enzyme inactivators. The so-called suicide-substrate strategies constitute a fascinating area of interdisciplinary research. We explain the procedure to represent mathematically how a hypothetical drug would act to inhibit the essential enzymes used by the SARS-CoV-2 virus to replicate and spread.

Considering the biological aspects and the mathematical applications presented in this article, the more relevant questions which arise are: 1) does the design of these drugs deserve a more detailed investigation? Could they be a viable alternative to the strategy of massive vaccine campaign against the SARS-CoV-2 virus?

Keywords: SARS-CoV-2, interleukin IL-6, anti-inflammatory mediators, enzymatic inhibition, suicide substrates, mathematical modeling, ordinary differential equations, fixed points, stability analysis, quasi-steady-state assumption, numerical simulations, experimental data

Citation: Bernuzzi, P, Esposito, R, Mascia, C, Massimi, A, Pallicca, F, Sanna, A, Simeoni, C, 2020, "COVID-19 calls for Mathematics, Part 2: Interleukin IL-6 and Myo-Inositol, Suicide-substrate Enzyme Inhibitors", *Organisms: Journal of Biological Sciences*, vol. 4, no. 1, pp. 128-139. DOI: 10.13133/2532-5876/16969.

1. Interleukin IL-6 and myo-Inositol

As the outbreak of SARS-CoV-2 spreads around the world, it is noted that most of the deceases attributed to the virus are actually caused by its consequent Acute Distress Respiratory Syndrome (ARDS). Comparing the present situation to other coronavirus infections, it seems possible that a deregulated response from cytokines constitutes the principal cause of this respiratory failure. Indeed, patients with severe SARS-CoV-2 typically display a cytokine storm syndrome, unleashed by CD4 T lymphocytes which become activated as T helper-1 cells [4]. The lungs are infiltrated by inflammatory cells, such as lymphocytes, and examinations on patients in critical condition show diffuse alveolar damage with exudates [34]. This also produces disruption in the interstitium and in crosstalk between cells, endangering oxygen exchanges. In fact, from previous studies on pathogenic coronavirus epidemics [6], the exuberant immune response by cytokines is known to induce apoptosis in both endothelial and epithelial cells, thus causing vascular leakage and alveolar oedema, ultimately resulting in hypoxia.

Particularly, the cytokine which seems to play a central role is interleukin IL-6, mainly because during cytokine storms the amount of other inflammatory cytokines is not comparable to the major boost observed in IL-6 production. It is thought that this pathological increase in IL-6 levels may be determined by the altered balance between Regnase-1 and Arid5a proteins in post-transcriptional modification of the IL-6 mRNA, and some studies indicate that Arid5a predominance over ribonuclease Regnase-1 promotes inflammatory processes [14, 25]. Furthermore, most patients incurring in respiratory failure are already affected by unfavorable medical conditions, such as hypertension, cardiovascular disorders and cancer, also associated with IL-6 high levels [10, 19], whose release can be exacerbated by the virus: as a matter of fact, these are the patients who demonstrate an adverse clinical outcome after hospitalization.

Everything thus far suggests that, in order to block the inflammatory storm, it is necessary to down-regulate specific cytokines, both by decreasing the rate of their production and increasing the rate of their destruction, and some promising clinical trials with tocilizumab, an IL-6 receptor inhibitor, have shown a significant improvement in patients clinical outcome [25, 1, 28]. Tocilizumab is a humanized anti-IL-6 receptor antibody which

blocks IL-6-mediated signal transduction by inhibiting IL-6 binding to transmembrane of the soluble IL-6 receptor (refer to Figure 4). However, as interleukin IL-6 plays an important role in both innate and adaptive immune response, clinical studies also revealed the insurgence of infections due to the use of IL-6 inhibitors [17].

As suggested by Bizzarri et al. [4], a valuable alternative to tocilizumab is provided by myo-Inositol, a naturally occurring polyol which has been proven to reduce IL-6 levels and to mitigate the inflammatory cascade, interestingly without peculiar side effects. Among the arguments for promoting the myo-Inositol as a possible remedy to IL-6-induced damages, its application for the treatment of Respiratory Distress Syndrome (RDS) in the newborn [11] and the beneficial effect against lung cancer [9] support its experimental administration in the combined treatment of other diseases of the upper and lower respiratory system, thus opening new perspectives for the case of SARS-CoV-2.

Mathematical modeling can considerably improve the understanding of endogenous mechanisms of inflammation and the delicate equilibrium between all participants in the human body immune response [13, 23, 15]. In particular, this methodological approach makes it possible to explore the circumstances which could lead to an excessive inflammation, hence resulting in tissue damage, organs dysfunction and possibly decease.

Contrary to previous models, such as the one advanced by Kumar et al. [13], where solely the pathogen and its pro-inflammatory mediators are taken into consideration, the model introduced by Reynolds et al. [23] aims to understand the robustness of the process with time-dependent anti-inflammatory mediators and to determine whether their utilization is advantageous. Anti-inflammatory mediators limit the harm caused to tissues by the inflammation and suppress the activity of phagocytes. Nevertheless, this action may have drawbacks, since too much efficiency would lead to a period of vulnerability of the immune system to pathogens: in fact, while exogenous anti-inflammation activity may impede the spreading of pro-inflammation agents and the tissue damage they would have induced, it also weakens the ensuing production of endogenous anti-inflammatory mediators [3, 2]. Thus, its effects on the outcome of pathogenic infections may be difficult to predict and, therefore, the problem requires a dynamical analysis such as the one presented in this article. The model proposed in [23] actually uses smaller subsy-

stems to build up more complex schemes, the smallest ones being coherent with the experimental results of previous studies and validated within the already known interaction between components of the immune response. For the cases discussed in Section 2, elements of the adaptive immune response are not included, such as specific antibodies, and also the anti-inflammatory mediators are not characterized.

The activation of anti-inflammatory mediators can be modeled by building a differential system in which P denotes the density of pathogen, N^* represents the activated phagocytes, D describes the amount of damaged tissue and C_A is the concentration of anti-inflammatory mediators. These variables evolve in time, and their growth depends non-linearly on the value of all the others. In particular, we consider the fact that phagocytes respond to the presence of a pathogen and try to eliminate it. Doing this causes collateral injuries, such as inflammation and damage to tissues, but the latter also activates more phagocytes, and therefore N^* and D actually fuel reciprocally. The anti-inflammatory mediators, such as interleukin IL-10 [22, 12], respond to the presence of activated phagocytes and other damages, and try to suppress them. A way to investigate more specifically the effects of C_A administration is to assign different functions which replicate the variation of anti-inflammatory mediators in time [23], in order to improve the clinical situation or at least avoid patients decease. This approach makes it possible to select the more plausible strategy to achieve favorable outcomes with the system returning to a stable healthy state.

At the first attempt, C_A can be seen as a parameter, constant in time. Then, the speed of evolution for P , N^* and D is simplified by considering various recurrent real life situations, to obtain the following system of nonlinear ordinary differential equations:

$$\begin{cases} \frac{dP}{dt} = k_{pg}P\left(1 - \frac{P}{p_\infty}\right) \\ \quad - \frac{k_{pm}s_mP}{\mu_m + k_{mp}P} - k_{pn}f(N^*)P \\ \frac{dN^*}{dt} = \frac{s_{nr}f(R)}{\mu_{nr} + f(R)} - \mu_n N^* \\ \frac{dD}{dt} = k_{dn}f_s(f(N^*)) - \mu_d D \end{cases} \quad (1)$$

where C_A appears implicitly through the definition of the reaction function, which is chosen as

$$f(V) = \frac{V}{1 + (C_A/c_\infty)^2}, \quad (2)$$

together with $f_s(V) = V^6/(x_{dn}^6 + V^6)$.

The action of anti-inflammatory mediators, as well as the inhibition of N^* and D , are represented by the linear (empirical) function f given in (2), which leaves its argument unchanged if C_A is null and diminishes constantly, tending to zero, if C_A is increasing.

The variation of P depends on its logistic growth, with rate k_{pg} ranging from 0.021 h^{-1} to 2.44 h^{-1} , which accounts for the reproduction of pathogen, but considering that an excessive amount (namely, above a given threshold p_∞) leads to more spontaneous self-deterioration. The second term in the first equation describes a non-specific local response, such as the action of tissue macrophages and other biological defenses. This activation is typically fast, i.e. occurring only during a short period of time, hence that term can be deduced by simplifying a smaller model under the quasi-steady-state assumption (QSSA) that the speed of the response is almost null [23]. Finally, the effect of activated phagocytes is incorporated through the last term and it depends on the interaction between the phagocytes themselves and the pathogen.

The second equation summarizes the speed of N^* in two terms. The first one considers the awakening of resting phagocytes, that is a rapid process, and in fact this term is obtained by simplifying another smaller model [23] again by means of the QSSA hypothesis. The auxiliary variable R grows linearly with the presence of P , N^* and D according to an empirical law [23], namely $R = k_{nr}N^* + k_{np}P + k_{nd}D$. Then, the second term illustrates the deterioration of activated phagocytes in time.

The temporal variation of D is represented in the last equation of system (1) and includes two terms. The S-shaped function f_s is intended to suggest that low amounts of phagocytes cause few damages to the surrounding tissue but, while increasing, the damage spreads until its saturation, meaning that it will not exceed a certain value (even in the presence of a large amount of phagocytes). Indeed, f_s is null if there are no activated phagocytes, and tends monotonically to a constant as shown in Figure 1. The last term imitates the spontaneous healing process of the system.

We point out that some of the parameters used to build the model (1) are the results of experimentation,

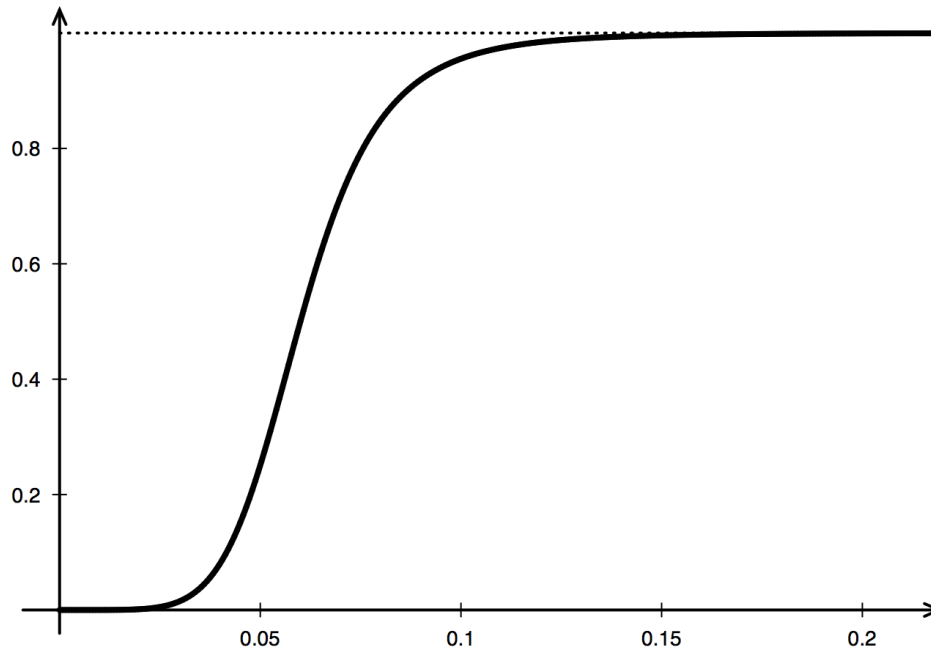


Figure 1: Graphic shape of the function f_s used to describe the speed of D in the model (1).

while others, and especially k_{pg} inside the first equation, are varied in order to study different situations (all their values are positive or null). Unless specified otherwise, the numerical values for the simulation parameters are those reported in Table 1.

parameters	values	units
p_∞	20	10^6 cc^{-1}
k_{pm}	0.6	$N^*\text{-units}^{-1} \text{ h}$
s_m	0.005	$N^*\text{-units} \text{ h}^{-1}$
μ_m	0.002	h^{-1}
k_{mp}	0.01	$P\text{-units}^{-1} \text{ h}$
k_{pn}	1.8	$N^*\text{-units}^{-1} \text{ h}$
s_{nr}	0.08	$N^*\text{-units} \text{ h}^{-1}$
μ_{nr}	0.12	h^{-1}
μ_n	0.05	h^{-1}
k_{dn}	0.35	$D\text{-units} \text{ h}^{-1}$
μ_d	0.02	h^{-1}
s_c	0.0125	$C_A\text{-units} \text{ h}^{-1}$
k_{cn}	0.04	$C_A\text{-units} \text{ h}^{-1}$
k_{cnd}	48	$N^*\text{-units} D\text{-units}^{-1}$
μ_c	0.1	h^{-1}
k_{nn}	0.01	$N^*\text{-units}^{-1} \text{ h}$
k_{np}	0.1	$P\text{-units}^{-1} \text{ h}$
k_{nd}	0.02	$D\text{-units}^{-1} \text{ h}$
c_∞	0.28	$C_A\text{-units}$
x_{dn}	0.06	$N^*\text{-units}$

Table 1: Numerical values for the simulation parameters (refer to [23] for more details).

By studying analytically the system (1), starting from the smaller models which led to its construction [23],

various (but at most three) *fixed points* are found according to different values of C_A and k_{pg} , whose existence and stability properties sensibly depend on these parameters. In particular, the fixed points are endowed with a *basin of attraction*, namely a region of attractiveness for the overall dynamics.

The so-called *health state* is reached when pathogen, phagocytes and tissue damage are all null, and the amount of anti-inflammatory mediators is a specific constant; it is stable only if k_{pg} is less than 1.5 h^{-1} , otherwise it is unstable. The *aseptic death state* is reached when the pathogen has been eradicated but the inflammation has not been stopped, so phagocytes and tissue damage have high values; it exists if C_A is smaller than 0.626 pg/ml and the region of its existence is divided into two parts by some value, depending on k_{pg} and ranging between 1.707 h^{-1} and 3.8 h^{-1} , which, if bigger than C_A , makes the *aseptic death state* stable. The *septic death state* is reached when the phagocytes have been unable to stop the pathogen growth; it exhibits stability if k_{pg} crosses a positive value, which decreases while C_A increases but is never bigger than 0.276 pg/ml . For more details about the regions of stability and their dependence upon the changing parameters C_A and k_{pg} , we refer to [23]. These results suggest that, even with the administration of anti-inflammatory mediators, the stability of a health state depends strictly on k_{pg} , namely the growth rate of pathogen, and thus any effective strategy must include a

combination of various treatments [22, 12, 20, 24].

Moreover, while increasing C_A leads to the aseptic death state becoming an unstable fixed point, it also makes the septic death state a more plausible outcome, as portrayed for the example in Figure 2, because it opens a period of time in which the pathogen is free to multiply.

Dealing with the presence of anti-inflammatory mediators as a time-dependent variable leads to a new model, which is a variant of the system (1) already studied in [23], with a fourth equation describing the speed of evolution of C_A as follows:

$$\frac{dC_A}{dt} = s_c + \frac{k_{cn}f(N^* + k_{cnd}D)}{1 + f(N^* + k_{cnd}D)} - \mu_c C_A, \quad (3)$$

where the first term indicates a constant source of anti-inflammation mediators, possibly provided by myo-Inositol [4], while the two others replicate its activation in response to the presence of activated phagocytes and tissue damage, and its deterioration in time, respectively.

Comparing the model (1), by fixing the constant C_A , with its variation by adding equation (3), for which C_A is given as initial value, and studying the relationship between k_{pg} and the initial amount of pathogen P_0 , a finer description of the stability for the case of an health state is possible. Indeed, when k_{pg} is large enough to represent a threat to the system, but it is also small enough to ensure stability, the basin of attraction of the fixed points is wider if we assume the evolution model (3). An example of this phenomenon is shown in Figure 3, and these results indicate that an adaptive administration of anti-inflammatory mediators makes the patients recovery more plausible.

Finally, the model outcomes underline the importance of both anti-inflammatory and inflammatory response rates, also suggesting that they should be carefully tuned to overcome the more critical scenarios and restore health. Furthermore, the numerical simulations point out the narrow compromise between administering anti-inflammatory mediators and hindering the immune response: experimental studies and simulations have stressed out the importance of quantity and timing of the administration of anti-inflammatory me-

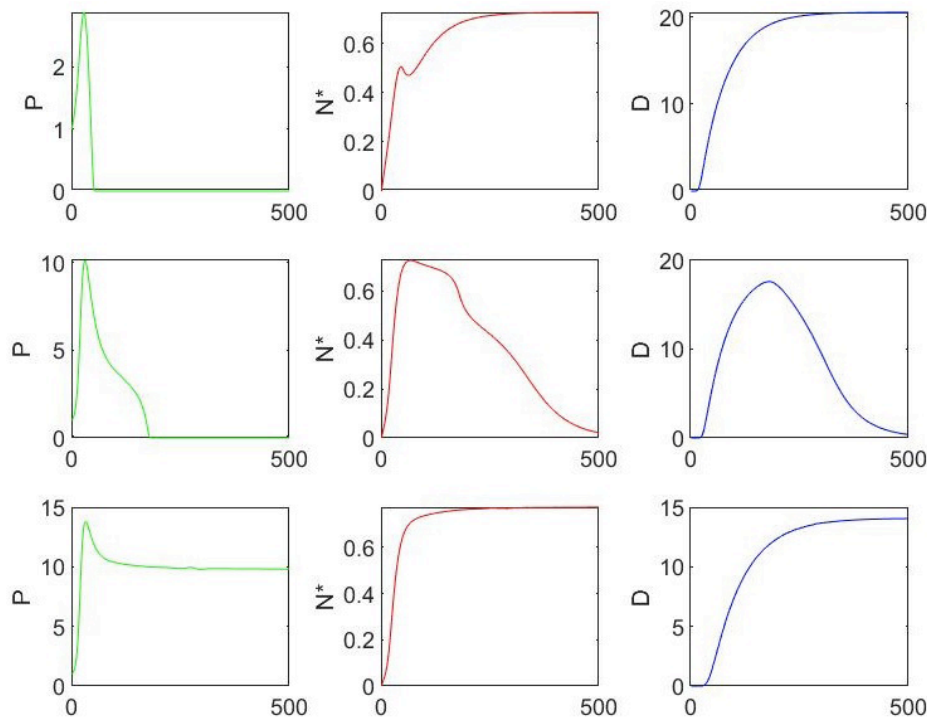


Figure 2: These graphs illustrate that, if k_{pg} is below 1.5 h^{-1} , the value of C_A plays an important role in the dynamics outcome. The results of three simulations of the model (1) are shown, with initial values $P = 1.0 \times 10^6 \text{ cc}^{-1}$, $N^* = D = 0$ and $k_{pg} = 0.3 \text{ h}^{-1}$, while C_A has different values (displayed according to the rows). The time, represented along the horizontal axis, is measured in hours, therefore the expected results are reported over three weeks. The first row graphs corresponds to $C_A = 0.5 \text{ pg/ml}$ and the outcome is the aseptic death, the second row corresponds to $C_A = 0.7 \text{ pg/ml}$ and the dynamics tends to the health state, while the third row corresponds to $C_A = 0.9 \text{ pg/ml}$ and represents the case of septic death.

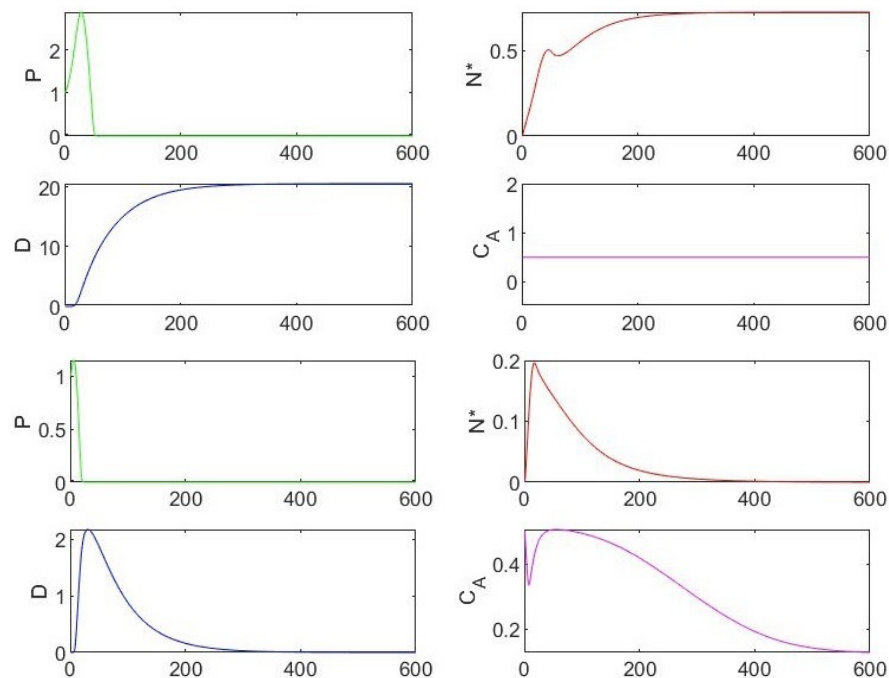


Figure 3: These graphs illustrate the expansion of the basin of attraction for the case of an health state. The first four charts correspond to the static model (1), while the others correspond to the dynamic case with additional equation (3). Both simulations start with $P_0 = 1.0106 \text{ cc}^{-1}$, $N^* = D = 0$ and $C_A = 0.5 \text{ pg/ml}$, as initial values, with the parameter $k_{pg} = 0.3 \text{ h}^{-1}$, but the outcome is very different. The first set of graphs shows the solution converging toward an aseptic death state, whilst the others indicate convergence toward a health state. These results estimate the recovery expectations in 25 days.

diators in patients whose clinical condition is on its way to a healthy resolution but has not reached it yet [3, 2].

However, the oversimplification of a complex problem is maybe the greatest downside of the models presented in this article, although their affordable size permitted a detailed analysis of emergent behaviors and the description of the principal catalysts involved in the process. Guidelines for future research include a more in-depth biological characterization of anti-inflammatory mediators for application to the SARS-CoV-2 virus, taking into account their specific activity and operational time-scale, and it might also be useful to incorporate a rigorous mathematical analysis to design efficient strategy for administrating therapeutic agents.

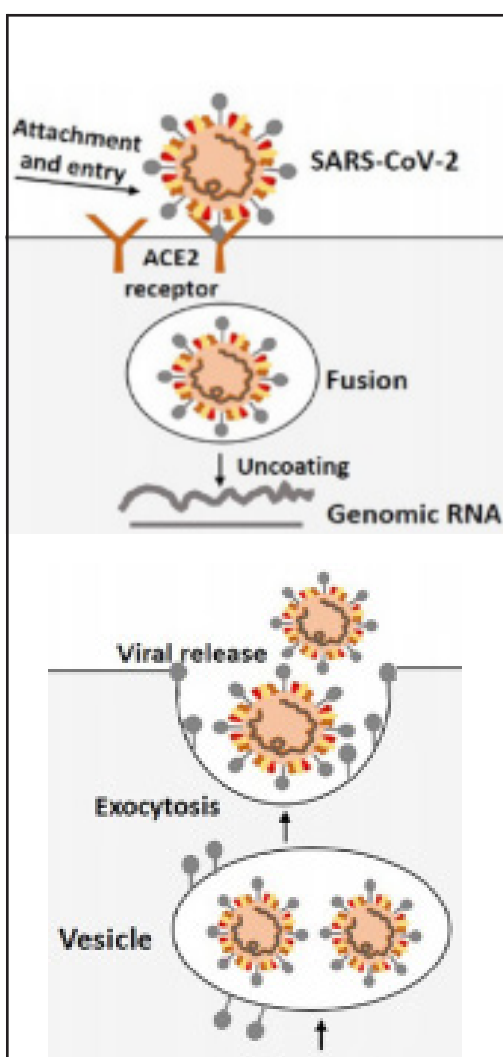
2. Suicide-substrate enzyme inhibitors

Coronaviruses are enveloped RNA viruses and include those which cause the common cold as well as the highly pathogenic Severe Acute Respiratory Syndrome coronaviruses (SARS-CoV) and Middle East Respiratory Syndrome coronaviruses (MERS-CoV). All coronaviruses contain specific genes which encode proteins for viral replication, nucleocapsid and spikes forma-

tion. The spike (S) glycoproteins on the outer surface of coronaviruses are responsible for the attachment and entry of the virus into host cells. The receptor-binding domain (RBD) is loosely attached to the virus particles and, therefore, the virus may actually infect multiple hosts. The entry mechanism of a coronavirus depends upon cellular proteases, including transmembrane protease serine 2 (TMPRSS2) which splits the S proteins and establish further penetration changes. SARS-coronaviruses require angiotensin-converting enzyme 2 (ACE2) as a key receptor. SARS-CoV-2 possesses the typical coronavirus structure with S proteins and also other polyproteins, nucleoproteins and membrane proteins. The transmission rate of SARS-CoV-2 is presently higher than that previously observed for SARS-CoV, and the reason could be some genetic recombination event occurring at S proteins inside the RBD region, which may have enhanced its transmission ability [24].

The life cycle of SARS-CoV-2 in host cells begins when S proteins bind to the ACE2 cellular receptor and the conformation changes induced into the S proteins facilitate viral envelope fusion with the cell membrane through the endosomal pathway (see Figure 4, above). Then SARS-CoV-2 releases its genomic RNA inside the

host cell, in order to be translated into active DNA used by the host cell to replicate the virus. The mechanism allowing this process is performed by the reverse transcriptase (RT) enzyme, whereas the nucleic acid of the virus is also exploited for the synthesis of viral proteins. Both viral proteins and genomic RNA are subsequently assembled into virions in the endoplasmic reticulum (ER) and Golgi, and finally transported via vesicles to be released out of the cells (see Figure 4, below).



Among the several candidate medicines which may inhibit infection and replication of SARS-CoV-2 [30,1, 4, 16, 24, 26], we focus our attention on the phenomenon of enzymatic inhibition through *mechanism-based enzyme inactivators* [7, 18]. There are two types of inhibition mechanisms employed by ligands for a specific protein: the irreversible inhibition is accompanied

by the formation of a covalent bond between the drug and its receptor, while the reversible inhibition is maintained by non-covalent intermolecular interactions. Binding of a reversible inhibitor would likely cause that one drug molecule hampers the activity of its target for a certain period; instead, binding of an irreversible inhibitor would generate a permanent bond between the drug and the related target macromolecule. In some cases of covalent inhibition, the enzyme also lends a hand to its own demise. Hence, the term “suicide” or “suicidal” inhibition—or rather mechanism-based inhibition—refers to that particular type where the enzyme prepares the ligand to commit suicide (these substrates are also called “Trojan horse inhibitors”). In recent years, suicidal inactivation has become a leading approach in studying enzyme-related mechanisms for rational designing of effective drugs in the pharmaceutical industry [7]. Physiologically, suicide-substrate systems target specific enzymes for inactivation, thereby reducing their activity, thus preventing substrate utilization and product formation [32, 31].

From a mathematical point of view, this process has been discussed in several studies [32, 31, 5, 27,8], which thoroughly analyze a modification of the classical *Michaelis-Menten* system shown in Figure 5, in order to account for the enzyme kinetics.

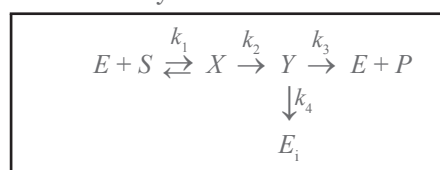


Figure 5: A simplified pathway of enzyme kinetics for suicide-substrate systems.

In that framework, the symbols E , S and P stand for enzyme, substrate and product, respectively, X and Y represent the enzyme-substrate intermediates, E_i denotes the inactivated enzyme, and all reactions are mediated by (positive) rate constants. Within such system, Y can follow two alternative pathways, namely toward $E+P$ with rate k_3 or toward E_i with rate k_4 . The quotient k_3/k_4 of these rates is called *partition ratio* and is usually denoted by r . Both pathways are considered to be irreversible over the time scale of the reaction. Then, irreversible inactivation of the enzyme implies that its form and functionality have been permanently modified; since it can no longer carry out its function, the enzyme thus commits suicide. The criteria for an inhibitor to be classified as *suicide substrate* include that inactivation

should be time-dependent, the reaction should be of first order type, and the enzyme should exhibit a saturation phenomenon [7].

The rate equations for the process illustrated in Figure 5 are deduced by means of the standard *law of mass action* as follows:

$$\left\{ \begin{array}{l} \frac{de}{dt} = -k_1 es + k_{-1} x + k_3 y \\ \frac{ds}{dt} = -k_1 es + k_{-1} x \\ \frac{dx}{dt} = k_1 es - k_{-1} x - k_2 x \\ \frac{dy}{dt} = k_2 x - k_3 y - k_4 y \\ \frac{de_i}{dt} = k_4 y \\ \frac{dp}{dt} = k_3 y \end{array} \right. \quad (4)$$

where e, s, x, y, e_i and p denote the chemical concentrations, as functions of the time. Typical experimental initial conditions completing this mathematical formulation are given by $e(0) = e_0, s(0) = s_0, x(0) = y(0) = e_i(0) = p(0) = 0$, for instance. Consequently, the system (4) is further simplified by adopting the following relations of mass conservation:

$$\left\{ \begin{array}{l} e_0 = e + x + y + e_i \\ s_0 = s + x + y + e_i + p \end{array} \right. \quad (5)$$

Moreover, the equation for p can be uncoupled from the others, because p does not appear in any other equation, hence p can be evaluated by direct integration after y has been computed. Finally, the reduced model obtained from (4) thanks to (5) contains only four coupled ordinary differential equations, namely

$$\left\{ \begin{array}{l} \frac{ds}{dt} = -k_1(e_0 - x - y - e_i)s + k_{-1}x \\ \frac{dx}{dt} = k_1(e_0 - x - y - e_i)s - (k_{-1} + k_2)x \\ \frac{dy}{dt} = k_2x - (k_3 + k_4)y \\ \frac{de_i}{dt} = k_4y \end{array} \right. \quad (6)$$

The quasi-steady-state assumption (QSSA) for the intermediate complexes, consisting in the hypothesis that $\frac{dx}{dt} = 0$ and $\frac{dy}{dt} = 0$ in system (6), yields an additio-

nal simplification, which implies the existence of explicit solutions given by

$$x = \frac{k_1 es}{k_{-1} + k_2}, \quad y = \frac{k_1 k_2 es}{(k_{-1} + k_2)(k_3 + k_4)}, \quad (7)$$

so that intermediate complexes computed from (7) bear the proportionality relation $x = Ky, K := \frac{k_2}{k_3 + k_4}$.

However, these equations are still too difficult to be solved analytically, without other simplifying approximations. Therefore, numerical simulations are carried out to illustrate some particular points. The biologically more relevant questions which arise are: 1) will all substrate be converted during the process? 2) will all the enzyme be inactivated? As indicated in [31], the factor determining whether the substrate is exhausted before all the enzyme is inactivated is $r \times m$, where m denotes the ratio of the initial concentrations of enzyme and substrate, namely e_0/s_0 . On the other hand, it is claimed in [27] that characteristic factor is $(1+r) \times m$, which is deduced by applying the conventional QSSA reduction method to obtain a two-dimensional system. In particular, when $(1+r) \times m \geq 1$, then the substrate is totally exhausted, whilst for $(1+r) \times m \leq 1$ all the enzyme is inactivated, so that both occur when $(1+r) \times m = 1$ (this result has been also achieved more recently in [8] without any QSSA simplifying hypothesis).

Although the results obtained in [27] seem to be more consistent with the numerical solutions to the full system of rate equations (4) than those presented in [31], both conclusions deviate from the solution when m approaches 1 (see Figure 6). This fact highlights a shortcoming of most QSSA approximations for enzyme kinetics, since their validity decreases for increasing values of the ratio e_0/s_0 . Consequently, a further analysis is needed because these indicators do not always lead to a correct conclusion.

For a quantitative estimation of the effectiveness of suicide substrates, a systematic mathematical study of these models may serve as an indicator to enzymologists, and especially to pharmacologists, during drugs administration and delivery, similarly to the methods applied for identifying indicators of suicidal inactivation in antibiotic kinetics (refer to [7] for more detailed information). In the scientific literature, there are few articles concerning the theoretical understanding of enzymatic reactions involving suicide substrates, possibly because of the severe lack of data from realistic ap-

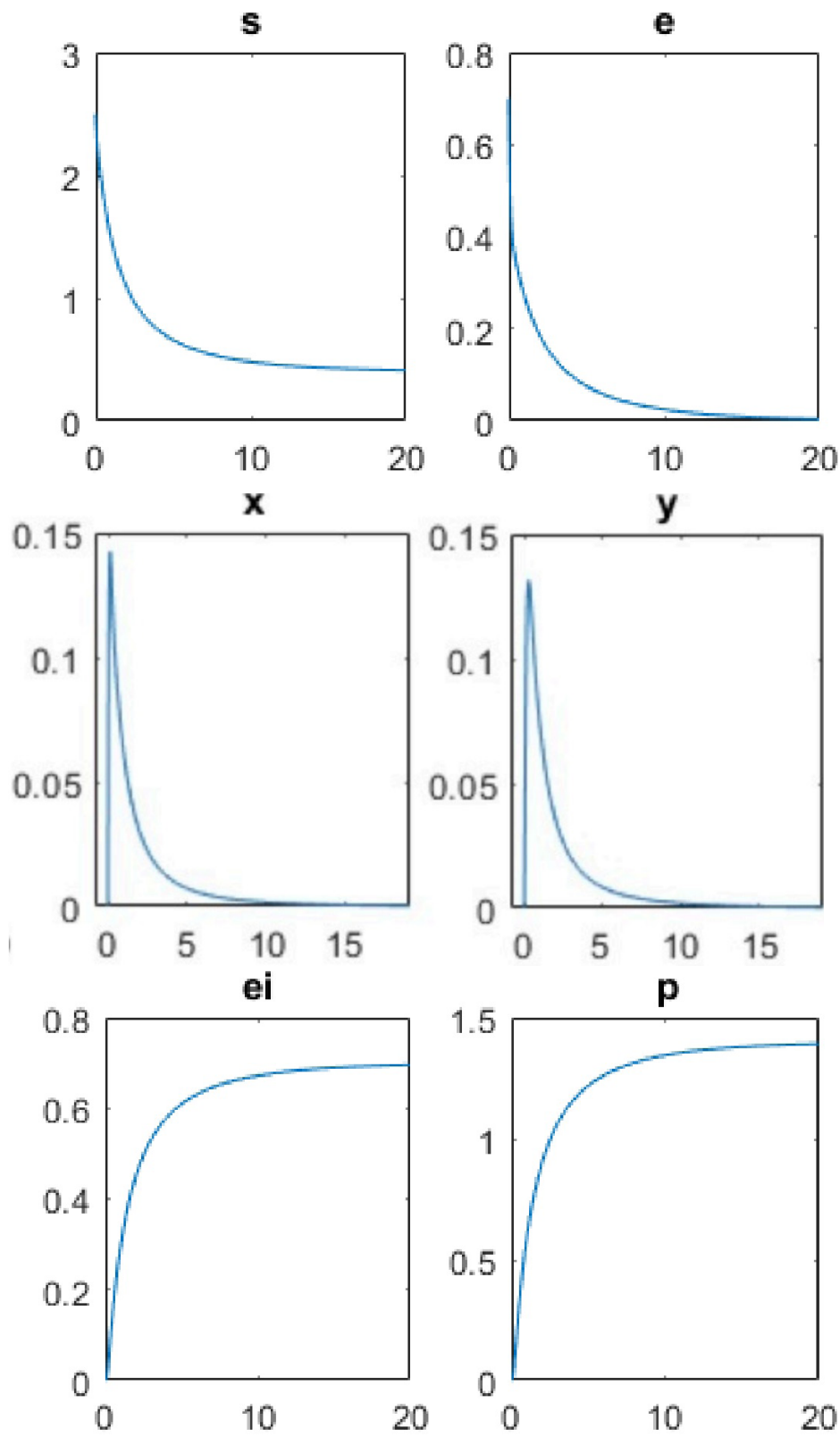


Figure 6: Temporal profiles for enzyme (e), substrate (s), intermediate complexes (x) and (y), product (p) and inactivated enzyme (e_i). The experimental data for numerical simulations are $e_0 = 0.7$, $s_0 = 2.5$, $k_1 = 2$, $k_{-1} = 4$, $k_2 = 10$, $k_3 = 6$, $k_4 = 3$, and these values are chosen to reproduce the case $(1+r) \times m < 1$. The curves show that all the enzyme is inactivated, and indeed the concentration e_i tends to e_0 , while there exists an excess of substrate. The intermediate complexes exhibit similar trends, characterized by an initial phase of rapid growth, before they rapidly run out toward the final product.

plications. Simultaneously, experimentalists are often holed up because of the lack of theoretical background to design experiments and perform a posteriori analysis of experimental data.

Several drugs acting as suicide inhibitors are currently demanded for the prevention and treatment of different diseases: popular clinical examples of suicide substrate therapies include Aspirin, Exemestane for the treatment of breast cancer, the azidothymidine (AZT) and other nucleoside analogues used against AIDS/HIV, Penicillin, etc. and have been also investigated for the treatment of depression (monoamine oxidase inhibitors) and epilepsy (inhibitors of brain GABA amino-transferase, for example).

Our hypothesis of suicide inhibition to neutralize the SARS-CoV-2 is not unfounded, since this approach has already been pursued in 2003 for the inactivation of the SARS-CoV Main proteinase (Mpro) by means of the benzotriazole esters [29, 21]. Indeed, the SARS-CoV-related Mpro plays a central role in the formation of the viral replicase/transcriptase complex and it appears to be an ideal target for the development of suitable drugs. The structure of complexes resulting from reaction of the SARS-CoV-related Mpro with two aromatic benzotriazole esters provided a promising starting point for designing more specific inhibitors for this proteinase [29]. Although benzotriazole esters, which act as suicide inhibitors, have been reported as potent non-peptidic inhibitors of the enzyme [33], their exact mechanism of action remains unclear. Unfortunately, the currently available protease inhibitor drugs do not seem to work correctly, and sometimes at all, for the treatment of SARS-CoV-2 virus. This is mainly due to the fact that proteases are a family of enzymes with many different characteristics and the drugs already developed for other pathologies are not perfectly compatible with specific proteases of the SARS-CoV-2 virus.

Of course, the creation of this type of drugs could be extremely beneficial, without neglecting different controversial aspects. Suicide-substrate inhibitors are harder to be identified and synthesized because they usually require a fully description of the enzymatic behavior for their design, to provide a base-structure target for the transition state of these enzymes. Due to their high potency and selectivity, as well as a lower propensity for the development of drug resistance, mechanism-based inhibitors can constitute a valuable outlook on the problem of drug resistance. Moreover, there are only a re-

stricted number of enzymes which are capable of being targeted by a mechanism-based inhibitor compared with thousands of synthetically feasible or available compounds in databases used by medicinal chemists. Suicide-substrate inhibitors are particularly invaluable for targeting proteins of bacterial cells when there is a low homology and similarity with human proteins, and the risk of toxicity is appreciably lower [18].

Acknowledgments

The authors thank the Department of Mathematics G. Castelnuovo, Sapienza University of Rome, for having hosted the electronic workshop COVID-19 calls for Mathematics —www1.mat.uniroma1.it/ricerca/convegni/2020/COVIDchiamaMAT – which has motivated this project. This project is partially supported by the French government, managed by the ANR under the UCA JEDI Investments for the Future project, reference no. ANR-15-IDEX-01.

References

1. Alattar, R, Ibrahim, TBH, Shaar, SH, Abdalla, S, Shukri, K, Daghdal, JN, Khatib, MY, Aboukamar, M, Abukhattab, M, Alsoub, HA, Almaslamani, MA & Omrani, AS 2020, “Tocilizumab for the treatment of severe coronavirus disease 2019”, *Journal of Medical Virology*, pp. 1-8.
2. Annane, D, Bellissant, E, Bollaert, PE, Briegel, J, Keh, D & Kupfer, Y, “Corticosteroids for treating sepsis (Review)”. *Cochrane Database of Systematic Reviews 2015*, vol. 12, Art. no. CD002243.
3. Annane, D, Sébille, V, Charpentier, C, Bollaert, PE, François, B, Korach, JM, Capellier, G, Cohen, Y, Azoulay, E, Troché, G, Chaumet-Riffaut, P & Bellissant, E 2002, “Effect of treatment with low doses of hydrocortisone and fludrocortisone on mortality in patients with septic shock”, *Journal of the American Medical Association*, vol. 288, no. 7, pp. 862-871.
4. Bizzarri, M, Laganà, AS, Aragona, D & Unfer V 2020, “Inositol and pulmonary function. Could myo-inositol treatment downregulate inflammation and cytokine release syndrome in SARS-CoV-2?”, *European Review for Medical and Pharmacological Sciences*, vol. 24, pp. 3426-3432.
5. Burke, MA, Maini, PK & Murray, JD 1990, “On the kinetics of suicide substrates”, *Biophysical Chemistry*, vol. 37, no. 1-3, pp. 81-90.
6. Channappanavar, R & Perlman S 2017, “Pathogenic human coronavirus infections: causes and

- consequences of cytokine storm and immunopathology”, *Seminars in Immunopathology*, vol. 39, no. 5, pp. 529-539.
7. Dhatt, S 2017, “Indicators for suicide substrate inactivation: a kinetic investigation”, *Journal of Chemical Sciences*, vol. 129, no. 12, pp. 1921-1928.
 8. Goeke A, Schilli C, Walcher S, Zerz, E 2012, “A note on the kinetics of suicide substrates”, *Journal of Mathematical Chemistry*, vol. 50, no. 6, pp. 1373-1377.
 9. Han, W, Gills, JJ, Memmott, RM, Lam, S & Dennis, PA 2009, “The chemopreventive agent myo-inositol inhibits Akt and extracellular signal-regulated kinase in bronchial lesions from heavy smokers” *Cancer Prevention Research*, vol. 2, pp. 370-376.
 10. Heinrich, PC, Behrmann, I, Haan, S, Hermanns, HM, Müller-Newen, G & Schaper, F 2003, “Principles of interleukin (IL)-6-type cytokine signalling and its regulation”, *Biochemical Journal*, vol. 374, no. 1, pp. 1-20.
 11. Howlett, A, Ohlsson, A & Plakkal, N 2012, “Inositol for respiratory distress syndrome in preterm infants”, *Cochrane Database of Systematic Reviews*, no.2, CD00036.
 12. Iyer, SS & Cheng, G 2012, “Role of Interleukin-10 transcriptional regulation of inflammation and autoimmune disease”, *Critical Reviews in Immunology*, vol. 32, no. 1, pp. 23-63.
 13. Kumar, R, Clermont, G, Vodovotz, Y & Chow, CC 2004, “The dynamics of acute inflammation”, *Journal of Theoretical Biology*, vol. 230, no. 2, pp. 145-155.
 14. Masuda, K, Ripley, B, Nishimura, R, Mino, T, Takeuchi, O, Shioi, G, Kiyonari, H & Kishimoto, T, “Arid5a controls IL-6 mRNA stability, which contributes to elevation of IL-6 level in vivo”, *Proceedings of the National Academy of Sciences of the United States of America*, vol. 110, no.23, pp. 9409-9414.
 15. Mathew, S, Bartels, J, Banerjee, I & Vodovotz, Y 2014, “Global sensitivity analysis of a mathematical model of acute inflammation identifies nonlinear dependence of cumulative tissue damage on host interleukin-6 responses”, *Journal of Theoretical Biology*, vol. 358, pp. 132-148.
 16. McKee, DL, Sternberg, A, Stange, U, Laufer, S & Naujokat, C 2020, “Candidate drugs against SARS-CoV-2 and COVID-19”, *Pharmacological Research*, vol.157, 104859.
 17. Morena, V, Milazzo, L, Oreni, L, Bestetti, G, Fossali T, Bassoli, C, Torre, A, Cossu, MV, Minari, C, Ballone, E, Perotti, A, Mileto, D, Niero, F, Merli S, Foschi, A, Vimercati, S, Rizzardini, G, Sollima, S, Bradanini, L, Galimberti, L, Colombo, R, Micheli, V, Negri, C, Ridolfo, AL, Meroni, L, Galli, M, Antinori, S & Corbellino, M 2020, “Off-label use of tocilizumab for the treatment of SARS-CoV-2 pneumonia in Milan, Italy”, *European Journal of Internal Medicine*, vol. 76, 36-42.
 18. Moshafi, MH, Ghasemshirazi, S & Abiri, A 2020. “The art of suicidal molecular seduction for targeting drug resistance” *Medical Hypotheses*, vol. 140, 109676.
 19. Nazari, F, Pearson, AT, Nör, JE & Jackson, TL 2018, “A mathematical model for IL-6-mediated, stem cell driven tumor growth and targeted treatment”, *PLoS Computational Biology*, vol. 14, no. 1, e1005920.
 20. Pelt, J, Busatto, S, Ferrari, M, Thompson, EA, Mody, K & Wolfram, J 2018, “Chloroquine and nanoparticle drug delivery: a promising combination”, *Pharmacology and Therapeutics*, vol. 191, pp. 43-49.
 21. Pillaiyar, T, Manickam, M, Namasivayam, V, Hayashi, Y & Jung, S-H 2016, “An overview of Severe Acute Respiratory Syndrome-coronavirus (SARS-CoV) 3CL protease inhibitors: Peptidomimetics and small molecule chemotherapy”, *Journal of Medicinal Chemistry*, vol. 59, no.14, pp. 6595-6628.
 22. Pretolani, M 1999, “Interleukin-10: an anti-inflammatory cytokine with therapeutic potential”, *Clinical and Experimental Allergy*, vol. 29, pp. 1164-1171.
 23. Reynolds, A, Rubin, J, Clermont, G, Day, J, Vodovotz, Y & Ermentraut, GB 2006, “A reduced mathematical model of the acute inflammatory response: I. Derivation of model and analysis of anti-inflammation”, *Journal of Theoretical Biology*, vol. 242, no. 1, pp. 220-236.
 24. Shereen, MA, Khan, S, Kazmi, A, Bashir, N & Siddique, R 2020, “COVID-19 infection: Origin, transmission, and characteristics of human coronaviruses”, *Journal of Advanced Research*, vol. 24, pp. 91-98.
 25. Tanaka, T, Narazaki, M & Kishimoto, T 2014, “IL-6 in Inflammation, Immunity and Disease”, *Cold Spring Harbor Perspectives in Biology*, vol. 6, 016295.
 26. Tarek, M & Savarino, A 2020, “Pharmacokinetic bases of the hydroxychloroquine response in COVID-19: implications for therapy and prevention”, medRxiv preprint <https://doi.org/10.1101/2020.04.23.20076471v1>
 27. Tatsunami, S, Yago, N & Hosoe, M 1981 \Kinetics of suicide substrates: Steady state treatments and computer-aided exact solutions”, *Biochimica et Biophysica Acta*, vol. 662, no. 2, pp. 226- 235.
 28. Toniati et al. 2020, “Tocilizumab for the treatment of severe COVID-19 pneumonia with hyperinflammatory syndrome and acute respiratory failure: A single center study of 100 patients

- in Brescia, Italy”, *Autoimmunity Reviews*, vol. 19, no. 7, 102568.
29. Verschueren, KH, Pumpor, K, Anemller, S, Chen, S, Mesters, JR & Hilgenfeld, R 2008, “A structural view of the inactivation of the SARS coronavirus main proteinase by benzotriazole esters”, *Chemistry & Biology*, vol. 15, no. 6, 597-606.
30. Vincent, MJ, Bergeron, E, Benjannet, S, Bobbie, RE, Rollin, PE, Ksiazek, TG, Seidah, NG & Nichol, ST 2005, “Chloroquine is a potential inhibitor of SARS coronavirus infection and spread”, *Virology Journal*, vol. 2, no. 69.
31. Waley, SG 1985, “Kinetics of suicide substrates. Practical procedures for determining parameters”, *Biochemical Journal*, vol. 227, no.3, pp. 843-849.
32. Walsh, CT 1984, “Suicide substrates, mechanism-based enzyme inactivators: recent developments”, *Annual Review of Biochemistry*, vol. 53, pp. 493-535.
33. Wu, CY, King, KY, Kuo CJ, Fang, JM, Wu YT, Ho, MY, Liao, CL, Shin, JJ, Liang, PH & Wong CY, 2006, “Stable benzotriazole esters as mechanism-based inactivators of the Severe Acute Respiratory Syndrome 3CL protease”, *Chemistry & Biology*, vol. 13, pp. 261-268.
34. Xu, Z, Shi, L, Wang, Y, Zhang, J, Huang, L, Zhang, C, Liu, S, Zhao, P, Liu, H, Zhu, L, Tai, Y, Bai, C, Gao, T, Song, J, Xia, P, Dong, J, Zhao, J & Wang FS 2020, “Pathological findings of COVID-19 associated with acute respiratory distress syndrome”, *The Lancet Respiratory Medicine*, vol. 8, no. 4, pp. 420-422.